

On the Sodium versus Iron Correlation in Late B-Type Stars *

Yoichi TAKEDA, Satoshi KAWANOMOTO, and Naoko OHISHI

National Astronomical Observatory, 2-21-1 Osawa, Mitaka, Tokyo 181-8588
takeda.yoichi@nao.ac.jp, kawanomoto.satoshi@nao.ac.jp, naoko.ohishi@nao.ac.jp

(Received 2013 August 20; accepted 2013 October 8)

Abstract

With an aim to study whether the close correlation between [Na/H] and [Fe/H] recently found in A-type stars further persists in the regime of B-type stars, the abundances of Na were determined for 30 selected sharp-lined late B-type stars ($10000 \text{ K} \lesssim T_{\text{eff}} \lesssim 14000 \text{ K}$) from the Na I 5890/5896 doublet. These Na abundances were then compared with the O and Fe abundances (derived from the O I 6156–8 and Fe II 6147/6149 lines) showing anti-correlated peculiarities. It turned out that, unlike the case of A-type stars, [Na/H] is roughly constant at a slightly sub-solar level ($[\text{Na}/\text{H}] \sim -0.2(\pm 0.2)$) without any significant correlation with [Fe/H] which shows considerable dispersion ranging from ~ -0.6 to $\sim +1.0$. This may serve as an important observational constraint for understanding the abundance peculiarities along with the physical mechanism of atomic diffusion in upper main-sequence stars of late A through late B-type including Am and HgMn stars.

Key words: physical processes: diffusion — stars: abundances
— stars: atmospheres — stars: chemically peculiar — stars: early-type

1. Introduction

Abundance studies of sodium (Na) for early-type stars in the upper main sequence have been insufficient, despite the astrophysical importance of this element. Actually, until recently, investigations of Na abundances have long been limited up to late A stars ($T_{\text{eff}} \lesssim 8500 \text{ K}$), and those of higher T_{eff} from early A through B remained essentially untouched.

This is presumably due to its elemental characteristics; i.e., an alkali element with only one valence electron weakly bound and thus its ionization potential is fairly low ($\sim 5.1 \text{ eV}$), which means that almost all Na atoms are ionized and only a very small fraction remain neutral in the atmospheres of early-type stars. Accordingly, several subordinate Na I lines of low

* Based on data collected at Okayama Astrophysical Observatory (NAOJ, Japan).

excitation ($\chi_{\text{low}} \sim 2$ eV) frequently used for abundance determinations in late-type FGK stars are too weak to be measurable at higher T_{eff} , while the strong resonance lines (Na I 5890/5896, so called D lines) tend to be avoided because they are not easy to handle (e.g., non-LTE effect, contamination of interstellar lines, strong parameter-sensitivity, etc.).

Nevertheless, an extensive Na abundance study based on non-LTE analysis of strong Na I 5890/5896 lines was challenged by Takeda et al. (2009; hereinafter referred to as Paper I) for 122 unbiased sample of A-type stars ($7000 \text{ K} \lesssim T_{\text{eff}} \lesssim 10000 \text{ K}$) having a wide range of rotational velocities. Unfortunately, the resulting abundances turned out systematically subsolar ($-1 \lesssim [\text{Na}/\text{H}] \lesssim 0$) and unreliable, which was eventually interpreted as due to the considerable sensitivity of Na abundances (derived from such strongly saturated Na I D lines) to a choice of microturbulence along with its inevitable uncertainty due to depth-dependence (see subsection 5.3 in Paper I and the references therein).

Having learned a lesson for this problem, Takeda et al. (2012; hereinafter referred to as Paper II) then determined the abundances of Na (along with other alkalis such as Li and K) based on weaker subordinate Na I 5682/5688 lines (less sensitive to microturbulence) for 24 selected sharp-lined A-type stars ($v_e \sin i \lesssim 50 \text{ km s}^{-1}$, $7000 \text{ K} \lesssim T_{\text{eff}} \lesssim 10000 \text{ K}$). Interestingly, the resulting Na abundances were found to tightly scale with those of Fe (cf. figure 11a in Paper II), despite that Fe abundances were quite diversified in those 24 sample stars including Am stars (generally showing Fe enrichment). Actually, this tendency is considered to hold for A-type stars in general, since figure 7b in Paper I definitely shows evidence of such a positive correlation (even if $[\text{Na}/\text{H}]$ values themselves may suffer systematic errors).

This correlation between Na and Fe has a significant implication on the understanding of the physical mechanism for producing the abundance anomalies of Am stars (a group of A-type stars generally of slow rotation; see, e.g., Preston 1974 for a review), where heavier elements such as iron-group are overabundant while light elements such as CNO tend to be deficient. It is generally believed that some kind of segregation process (atomic diffusion) in the stellar envelope (depending on the balance between the downward gravitational settlement and upward radiative acceleration) is responsible for these peculiarities. However, since none of the existing theoretical calculations for Am stars (e.g., Richer et al. 2000 or Talon et al. 2006) has predicted that Fe and Na behave in the same way, this observational facts may require that the theory should be improved. How come these two elements (where atomic level configurations considerably differ from each other) show similar anomalies?

Here, we should recall that another group of apparently non-magnetic chemically peculiar stars of somewhat higher T_{eff} exists at the spectral type of late B, which are namely HgMn stars (cf. the review by Preston 1974) sharing rather similar characteristics to those of Am stars; such as an underabundance of O coupled with an overabundance of Fe (e.g., Takeda et al. 1999). Actually, the possible connection between these two groups has been occasionally argued (e.g., Adelman, Adelman, & Pintado 2003). If so, it is worthwhile to check whether

or not such a close correlation between Na and Fe is seen also in sharp-lined late B-type stars including HgMn stars.

As already mentioned, very few people have tried determinations of Na abundances for B-type stars so far, except for the recent LTE studies of Fossati et al. (2009) for two sharp-lined late-B stars (21 Peg and π Cet). Given this situation, we decided to carry out a new spectroscopic study for the abundances of O, Fe, and Na (where O and Fe abundances are indicators for HgMn peculiarities) for selected 30 sharp-lined late B-type stars, with an aim to give a clear answer to this question (i.e., whether or not Na correlates with Fe also in late B-type stars). This time, since subordinate lines such as Na I 5682/5688 are too weak to be measurable, we have no other way than to invoke the resonance lines of Na I 5890/5896, which are fortunately moderately weak and not strongly saturated at this range of T_{eff} ; thus, we do not suffer such problems as encountered in Paper I. The purpose of this paper is to report the outcome of this investigation.

2. Observational Data

As the targets of this study, we selected 30 late B-type stars (including a few A0 stars) mostly with spectral classes of B6–B9.5 and luminosity classes of III–V (cf. table 1), which are comparatively sharp-lined for early-type stars ($v_e \sin i \lesssim 60 \text{ km s}^{-1}$).

For 9 stars among these, we could avail ourselves of old spectra covering a wavelength range of 5600–6800 Å with a resolving power of $R \sim 70000$, which were obtained in 2006 October by using HIDES spectrograph at Okayama Astrophysical Observatory (OAO) to determine the O and Ne abundances of B-type stars. See Takeda et al. (2010) for more details.

Regarding the other 21 stars, we carried out new observations on 2012 May 26–31 again by using OAO/HIDES, where the same slit width (200 μm) as in 2006 October observations was adopted to get spectra of $R \sim 70000$ covering the wavelength range of 5100–8800 Å.¹ The reduction of these new 2012 spectra was done in the same manner as in 2006 data, and S/N ratios typically on the order of ~ 200 were attained. For both of the 2006 and 2012 data, telluric lines existing in the region of Na I 5890/5896 lines were removed by dividing the spectra by that of a rapid rotator as done in Paper I.

These 30 program stars are plotted on the $\log L$ vs. $\log T_{\text{eff}}$ diagram (theoretical HR diagram) in figure 1, where Girardi et al.’s (2000) theoretical evolutionary tracks corresponding to different stellar masses are also depicted. We can see from this figure that the masses of our sample stars are in the range between $\sim 2.5M_{\odot}$ and $\sim 5M_{\odot}$.

¹ Note that at the time of 2006 observation, the wavelength coverage of HIDES was only ~ 1200 Å because only one CCD was available. At present, HIDES has three mosaicked 4K \times 2K CCDs, accomplishing the whole wavelength coverage of ~ 3700 Å in the mode of red cross-disperser.

3. Atmospheric Parameters

In order to maintain consistency with our recent studies (Paper I, Paper II, Takeda et al. 2010), the effective temperature (T_{eff}) and the surface gravity ($\log g$) of each program star were determined from the colors of Strömberg’s *uvby β* photometric system with the help of Napiwotzki, Schönberner, and Wenske’s (1993) *uvbybetanew* program², where the observational data of $b - y$, c_1 , m_1 , and β were taken from Hauck and Mermilliod (1998) via the SIMBAD database. The resulting T_{eff} and $\log g$ are summarized in table 1. Their typical errors may be estimated as $\sim 3\%$ in T_{eff} and ~ 0.2 dex in $\log g$ for the present case of late B stars, according to Napiwotzki et al. (1993; cf. their section 5).³

The model atmosphere for each star was then constructed by two-dimensionally interpolating Kurucz’s (1993) ATLAS9 model grid in terms of T_{eff} and $\log g$, where the solar-metallicity models were exclusively used as in our previous studies.

Regarding the microturbulent velocity (ξ), we assume $\xi = 1 \text{ km s}^{-1}$ with uncertainties of $\pm 1 \text{ km s}^{-1}$ in this study,⁴ which we regard as most reasonable considering the published ξ results for late B-type stars ($10000 \text{ K} \lesssim T_{\text{eff}} \lesssim 15000 \text{ K}$) typically ranging between ~ 0 and $\sim 2 \text{ km s}^{-1}$ (see, e.g., table 1 of Sadakane 1990).

4. Abundance Determinations

The determination procedures of elemental abundances and related quantities (e.g., non-LTE correction, uncertainties due to ambiguities of atmospheric parameters) are essentially the same as adopted in Takeda et al. (1999), Papers I and II, and Takeda et al. (2010), which consist of two consecutive steps.

4.1. Synthetic spectrum fitting

The first step is to find the solutions for the abundances of relevant elements, projected rotational velocity ($v_e \sin i$), and radial velocity (V_{rad}) such as those accomplishing the best fit (minimizing $O - C$ residuals) between theoretical and observed spectra, while applying the automatic fitting algorithm (Takeda 1995). Two wavelength regions were selected for this

² (<http://www.astro.le.ac.uk/~rn38/uvbybeta.html>).

³ As a check, we also tried deriving T_{eff} and $\log g$ by using Moon’s (1985) UVBYBETA/TEFFLOGG program based on Moon and Dworetzky’s (1985) calibration, which may be better for stars of the relevant spectral type according to Kaiser (2006). We then found that the resulting values of T_{eff} are slightly (but systematically) higher by $\sim 200 \text{ K}$ ($\langle \Delta T_{\text{eff}} \rangle = 208 \pm 124 \text{ K}$) while those of $\log g$ are practically the same ($\langle \Delta \log g \rangle = -0.03 \pm 0.05 \text{ dex}$), compared to our adopted parameters based on the Napiwotzki et al.’s (1993) *uvbybetanew* program. Therefore, we should bear in mind the possibility that our T_{eff} given in table 1 might be slightly underestimated by $\sim 200 \text{ K}$ on the average, though this is still within the considered uncertainty ($\sim \pm 3\%$).

⁴ In contrast, Takeda et al. (2010) assumed $\xi = 3 \text{ km s}^{-1}$ with uncertainties of $\pm 2 \text{ km s}^{-1}$ based on the results of Lyubimkov, Rostopchin, and Lambert (2004), since B-type main-sequence stars in a much wider T_{eff} range ($10000 \text{ K} \lesssim T_{\text{eff}} \lesssim 23000 \text{ K}$, corresponding to masses of 4–11 M_{\odot}) were involved in that investigation.

purpose: [1] 6145–6160 Å region comprising O I 6156–8 and Fe II 6147/6149 lines, which is to determine the abundances of oxygen and iron, and [2] 5888–5898 Å region comprising Na I 5890/5896 lines to establish the abundance of Na. The adopted atomic data of important lines are presented in table 2. How the theoretical spectrum for the converged solutions fits well with the observed spectrum is displayed in figures 2 (region [1]) and 3 (region [2]). The $v_e \sin i$ values⁵ resulting from region [1] fitting are presented in table 1.

Note that, in the evaluation of $O - C$ residuals, we had to occasionally mask some regions showing features irrelevant to stellar spectra; such as spurious spectrum defect (figure 2) or interstellar absorption components of Na I 5890/5896 lines (figure 3), as highlighted in green in both figures. Also, in the case of 5888–5898 Å fitting of Na I lines, $v_e \sin i$ values were often fixed at the values derived from 6145–6160 Å fitting, since only incomplete Na I D line profiles are available in most cases.

4.2. Analysis on inversely evaluated W_λ

As the second step, with the help of Kurucz’s (1993) WIDTH9 program (which had been considerably modified in various respects; e.g., inclusion of non-LTE effects, treatment of total equivalent width for multi-component lines; etc.), we computed the equivalent widths of the representative lines “inversely” from the abundance solutions (resulting from spectrum synthesis) along with the adopted atmospheric model/parameters; i.e., W_{6147}^{Fe} (for Fe II 6147), W_{6156-8}^{O} (for O I 6156–8 merged triplet), and W_{5890}^{Na} (for Na I 5890).

Since the non-LTE effect was explicitly taken into consideration for O and Na as done in Papers I, II, and Takeda et al. (1999, 2010), A_N (NLTE abundance) and A_L (LTE abundance) were computed from W_{6156-8}^{O} and W_{5890}^{Na} , from which the NLTE correction Δ ($\equiv A_N - A_L$) was further derived. The resulting NLTE abundances and corrections for O and Na, as well as the LTE abundances for Fe, are given in table 1. Although only the results for the stronger Na I 5890 line of the doublet are given in table 1, those for the weaker Na I 5896 are well represented by the following formula:

$$W_{5896} = 6.74 \times 10^{-1} + 4.68 \times 10^{-1} W_{5890} + 2.96 \times 10^{-3} W_{5890}^2 \quad (1)$$

where W_{5896} and W_{5890} are measured in mÅ, and

$$\Delta_{5896} = -0.268 - 0.254 \Delta_{5890} - 0.946 \Delta_{5890}^2. \quad (2)$$

As expected, inequality relations of $W_{5896} < W_{5890}$ and $|\Delta_{5896}| < |\Delta_{5890}|$ generally hold.

We then estimated six kinds of abundance variations (δ_{T+} , δ_{T-} , δ_{g+} , δ_{g-} , $\delta_{\xi+}$, and $\delta_{\xi-}$)

⁵ It should be kept in mind that we assumed only the rotational broadening (with the limb-darkening coefficient of $\epsilon = 0.5$) as the macrobroadening function to be convolved with the intrinsic theoretical line profiles. Accordingly, $v_e \sin i$ values for very sharp-line cases (e.g., $v_e \sin i \lesssim 5\text{--}6 \text{ km s}^{-1}$) may be somewhat overestimated because the effects of the instrumental broadening or of the macroturbulence may not be negligible compared to $v_e \sin i$.

for A^{O} , A^{Na} , and A^{Fe} by repeating the analysis on the W values while perturbing the standard atmospheric parameters interchangeably by $\pm 3\%$ in T_{eff} , ± 0.2 dex in $\log g$, and ± 1 km s $^{-1}$ in ξ (which are the typical ambiguities of the parameters we adopted; cf. section 3). Finally, the root-sum-square of these perturbations, $\delta_{Tg\xi} \equiv (\delta_T^2 + \delta_g^2 + \delta_\xi^2)^{1/2}$, were regarded as abundance uncertainties (due to combined errors in T_{eff} , $\log g$, and ξ), where δ_T , δ_g , and δ_ξ are defined as $\delta_T \equiv (|\delta_{T+}| + |\delta_{T-}|)/2$, $\delta_g \equiv (|\delta_{g+}| + |\delta_{g-}|)/2$, and $\delta_\xi \equiv (|\delta_{\xi+}| + |\delta_{\xi-}|)/2$, respectively.

Figures 4(O), 5(Na), and 6(Fe) graphically show the resulting abundances, equivalent widths, non-LTE corrections (or $v_e \sin i$ in figure 6), and abundance variations in response to parameter changes, as functions of T_{eff} . We can see from these figures that, while the extents of non-LTE corrections for O I 6156–8 are not very significant (typically ~ 0.1 – 0.2 dex), those for Na I 5890 are significantly large and non-negligible (~ 0.3 – 0.5 dex). Besides, the abundance errors due to parameter uncertainties are typically ~ 0.1 – 0.2 dex for Na and Fe (though errors in Na may grow up to $\lesssim 0.3$ dex for near-A0 stars with $T_{\text{eff}} \lesssim 11000$ K), while those for O are not important ($\lesssim 0.1$ dex).

5. Discussion

5.1. Trend of O/Na/Fe Abundances with $v_e \sin i$

In order to discuss the results derived in section 4, the mutual relations between $[\text{O}/\text{H}]$, $[\text{Na}/\text{H}]$, and $[\text{Fe}/\text{H}]$ (the differential abundances relative to the Sun) as well as their behaviors with respect to $v_e \sin i$ are displayed in figure 7, where stars with $T_{\text{eff}} < 11000$ K and $T_{\text{eff}} > 11000$ K are discriminated in different symbols.

We can barely recognize the weak $v_e \sin i$ -dependence in $[\text{O}/\text{H}]$ (figure 7d) and $[\text{Fe}/\text{H}]$ (figure 7f) (i.e., O tends to be deficient while Fe to be overabundant with a decrease in $v_e \sin i$). Besides, figure 7a manifestly shows that $[\text{O}/\text{H}]$ and $[\text{Fe}/\text{H}]$ are anti-correlated with each other in the sense that $[\text{O}/\text{H}]$ gets decreased from ~ 0.0 to ~ -0.7 as $[\text{Fe}/\text{H}]$ increases from ~ 0.0 to $\sim +1.0$. Since these tendencies are qualitatively the same as seen in sharp-lined A-type stars showing Am phenomenon (Takeda & Sadakane 1997, Takeda et al. 2008, Paper I), we may state that O and Fe abundances of these sharp-lined late B-type stars (10000 K $\lesssim T_{\text{eff}} \lesssim 14000$ K) can be regarded as peculiarity indicators (weakly dependent upon $v_e \sin i$, behaving in an opposite way to each other) just as has been reported for A-type stars (7000 K $\lesssim T_{\text{eff}} \lesssim 10000$ K). Note that this consequence is consistent with the results of Takeda et al. (1999; cf. figures 10 and 11 therein)

Now, we are almost ready to answer the question which originally motivated this investigation: “Does $[\text{Na}/\text{H}]$ scale with $[\text{Fe}/\text{H}]$ in accordance with the extent of peculiarity in these late B stars, just as seen in A stars?” Our answer is negative according to figure 7b, which reveals that $[\text{Na}/\text{H}]$ values are roughly homogeneous distributing at a mildly subsolar level between ~ -0.5 and ~ 0.0 (the average is $\langle [\text{Na}/\text{H}] \rangle = -0.19$ with $\sigma = 0.16$, where the

outlier value of $[\text{Na}/\text{H}] = +0.59$ for HD 143807⁶ is excluded) without any significant dependence on $[\text{Fe}/\text{H}]$ (showing a large dispersion from ~ -0.6 to $\sim +1.0$). Yet, if we confine to stars with $10000 \text{ K} \lesssim T_{\text{eff}} \lesssim 11000 \text{ K}$ (red circles in figure 7b), we still see a sign of weak positive correlation between $[\text{Na}/\text{H}]$ and $[\text{Fe}/\text{H}]$, presumably because they tend to share the characteristics of A0-type stars. However, as T_{eff} becomes higher, this trend eventually disappears at $T_{\text{eff}} \gtrsim 11000 \text{ K}$ (blue triangles) where $[\text{Na}/\text{H}]$ tends to be stabilized with only a small dispersion around $[\text{Na}/\text{H}] \sim -0.2 (\pm 0.2)$. Hence, we may state that whether and how Na correlate with Fe in upper main-sequence stars depends significantly on T_{eff} .

5.2. T_{eff} -Dependence of Na vs. Fe Correlation

Let us investigate this issue in a more quantitative manner. Combining the present results with those of our previous studies (Takeda 2007; Paper II), we display in figure 8 the $[\text{Na}/\text{H}]$ vs. $[\text{Fe}/\text{H}]$ relations for four stellar groups of different T_{eff} ranges (FGK-type stars, A-type stars, late B-type stars of near A0, and late B-type stars), and the statistical quantities showing the nature of correlation between these two elements were also computed for each group as given in table 3. We can recognize from this table (and intuitively confirmed from figure 8) that the slope (m) of linear-regression relation ($[\text{Na}/\text{H}] \sim m [\text{Fe}/\text{H}] + b$) progressively decreases while the dispersion increases as T_{eff} becomes higher, which is an interesting tendency. It should be remarked, however, that the characteristics of FGK stars (first group) and those of A–B stars (last three groups) are intrinsically different from each other.

Regarding the former late-type stars in the Galactic disk ($\sim 1\text{--}1.5 M_{\odot}$) which have ages of $\sim 10^9\text{--}10^{10}$ yr, the reason for the spread of ~ 1 dex in $[\text{Fe}/\text{H}]$ as well as $[\text{Na}/\text{H}]$ is due to the chemical evolution in our Galaxy. And the scaling relation of $[\text{Na}/\text{H}] \sim [\text{Fe}/\text{H}]$ may be interpreted by the fact that the synthesis of Na (odd-Z neutron-rich element) is sensitive to neutron excess and thus considered to be metallicity-dependent. Actually, $[\text{Na}/\text{Fe}] \sim 0$ almost holds for disk stars of $-1 \lesssim [\text{Fe}/\text{H}] \lesssim 0$, though a slight upturn is observed at the metal-rich end ($0 \lesssim [\text{Fe}/\text{H}] \lesssim 0.5$) (see, e.g., Takeda et al. 2003).

In contrast, early-type stars with masses of $\sim 1.5\text{--}5 M_{\odot}$ are considerably younger ($\lesssim 10^8\text{--}10^9$ yr), which are regarded to have formed from gas of nearly the same chemical composition. (see, e.g., the near-homogeneity of O and Ne abundances in B-type stars derived by Takeda et al. 2010). Accordingly, the diversified Na as well as Fe abundances in these sharp-lined A and late-B stars ($T_{\text{eff}} \sim 7000\text{--}14000 \text{ K}$) must be due to “abundance peculiarities” which were acquired during their main-sequence life time presumably due to chemical segregation processes operating in the stable atmosphere or envelope. The significance of the result we found is, therefore, that

⁶ This star (ι CrB), being very sharp-lined with almost the lowest $v_e \sin i$ (4 km s^{-1}), belongs to the low T_{eff} group of near A0 (10828 K). Reflecting its conspicuously strong and saturated W_{5890} (116 m\AA), the Na abundance of this star is especially sensitive to errors in T_{eff} as well as ξ , as manifestly seen in figures 5d and 5f. Accordingly, we have to keep in mind that the Na abundance derived for this star is less reliable compared to other stars, which might explain (at least partly) this outlier nature.

it can provide with important observational characteristics of chemical peculiarities in A and late-B stars to be explained theoretically, e.g., by atomic diffusion calculations.

5.3. Conclusion

Regarding our primary aim of this investigation (i.e., to check whether or not the trend of Na vs. Fe correlation seen A-type stars persists into the regime of late B-type stars), our conclusion is summarized as follows:

— (1) In the regime of A-type stars ($7000 \text{ K} \lesssim T_{\text{eff}} \lesssim 10000 \text{ K}$), the mechanism causing chemical peculiarities (mainly Am anomalies in this case, characterized by overabundance of Fe and underabundance of O) acts nearly equally on both Na and Fe, so that a near-scaling relation between $[\text{Na}/\text{H}]$ and $[\text{Fe}/\text{H}]$ ($[\text{Na}/\text{H}] \sim 0.64 [\text{Fe}/\text{H}]$) is realized despite that these two elements have suffered appreciable abundance changes.

— (2) However, as T_{eff} is increased (higher than 10000 K), this relation first becomes appreciably loosened and ambiguous at the transition region ($10000 \text{ K} \lesssim T_{\text{eff}} \lesssim 11000 \text{ K}$), then the correlation eventually disappears at $11000 \text{ K} \lesssim T_{\text{eff}} \lesssim 14000 \text{ K}$ where $[\text{Na}/\text{H}]$ stabilizes almost at the primordial value⁷, despite both O and Fe still show $v_e \sin i$ -dependent anomalies. This suggests that the physical process causing abundance peculiarities does not work any more on Na at this higher- T_{eff} regime of late B-type stars, though it still operates on both Fe and O (typically exhibited by HgMn stars).

— (3) It is interesting to note that the “transition region” stars at $10000 \text{ K} \lesssim T_{\text{eff}} \lesssim 11000 \text{ K}$ are in the mass range of $2.5\text{--}3 M_{\odot}$ (cf. figure 1), which just correspond to the region on the HR diagram occupied by both HgMn stars and hot Am stars nearly overlapped as pointed out by Adelman et al. (2003; cf. figure 1 therein). We may state that these two groups of non-magnetic chemically peculiar stars (Am stars and HgMn stars) could be roughly characterized by the existence of Na–Fe correlation (i.e., both elements undergo abundance peculiarities in a similar manner) and the absence of such connection (i.e., Fe suffers anomaly while Na do not), respectively.

This consequence may serve as an important observational constraint for understanding the mechanism producing abundance peculiarities in upper main-sequence stars. Generally, less attention seems to have been paid to Na in early-type chemically peculiar stars, presumably because published observational data have been insufficient. Above all, diffusion calculations for Na in the envelope of B-type stars with $M \gtrsim 2.5 M_{\odot}$ seem to have been rarely conducted so far, except for the old work (e.g., Michaud et al. 1976). In this respect, new contributions by theoreticians are desirably expected toward reasonably explaining the observational trend for

⁷ Considering the near-homogeneity of these Na abundance without significant diversity, we tend to regard that primordial Na abundances (when stars were formed) are retained in the atmospheres of these stars at $T_{\text{eff}} \gtrsim 11000 \text{ K}$. As a matter of fact, we are not certain whether the slightly subsolar tendency in $[\text{Na}/\text{H}]$ (by ~ 0.2 dex on the average) is really meaningful, considering the possibility that our T_{eff} scale might as well be systematically raised by $\sim 200 \text{ K}$ (cf. footnote 3).

Na (along with O and Fe) confirmed in this investigation.

This research has made use of the SIMBAD database, operated by CDS, Strasbourg, France.

References

- Adelman, S. J., Adelman, A. S., & Pintado, O. I. 2003, *A&A*, 397, 267
- Arenou, F., Grenon, M., & Gómez, A. 1992, *A&A*, 258, 104
- Flower, P. J. 1996, *ApJ*, 469, 355
- Fossati, L., Ryabchikova, T., Bagnulo, S., Alecian, E., Grunhut, J., Kochukhov, O., & Wade, G. 2009, *A&A*, 503, 945
- Girardi, L., Bressan, A., Bertelli, G., & Chiosi, C. 2000, *A&AS*, 141, 371
- Hauck, B., & Mermilliod, M. 1998, *A&AS*, 129, 431
- Kaiser, A. 2006, in *Astrophysics of Variable Stars*, eds. C. Sterken & C. Aerts, *ASP Conf. Ser.* 349 (ASP: San Francisco), 257
- Kurucz, R. L. 1993, Kurucz CD-ROM, No. 13 (Harvard-Smithsonian Center for Astrophysics)
- Kurucz, R. L., & Bell, B. 1995, Kurucz CD-ROM, No. 23 (Harvard-Smithsonian Center for Astrophysics)
- Lyubimkov, L. S., Rostopchin, S. I., & Lambert, D. L. 2004, *MNRAS*, 351, 745
- Michaud, G., Charland, Y., Vauclair, S., Vauclair, G. 1976, *ApJ*, 210, 447
- Moon, T. T. 1985, *Commun. Univ. London Obs.*, No. 78
- Moon, T. T., & Dworetzky, M. M. 1985, *MNRAS*, 217, 305
- Moore, C. E. 1959, *A Multiplet Table of Astrophysical Interest: NBS Technical Note No. 36*, Reprinted Version of the 1945 edition (Washington, D. C., U. S. Department of Commerce)
- Napiwotzki, R., Schönberner, D., & Wenske, V. 1993, *A&A*, 268, 653
- Preston, G. W. 1974, *ARA&A*, 12, 257
- Richer, J., Michaud, G., & Turcotte, S. 2000, *ApJ*, 529, 338
- Sadakane, K. 1990, in *Lecture Note in Physics*, 357, *Accuracy of element abundances from stellar atmospheres* (Berlin: Springer), p.57
- Takeda, Y. 1995, *PASJ*, 47, 287
- Takeda, Y. 2007, *PASJ*, 59, 335
- Takeda, Y., Zhao, G., Takada-Hidai, M., Chen, Y.-Q., Saito, Y., & Zhang, H.-W. 2003, *ChJAA*, 3, 316
- Takeda, Y., Han, I., Kang, D.-I., Lee, B.-C., & Kim, K.-M. 2008, *JKAS*, 41, 83
- Takeda, Y., Kambe, E., Sadakane, K., & Masuda, S. 2010, *PASJ*, 62, 1239
- Takeda, Y., Kang, D.-I., Han, I., Lee, B.-C., & Kim, K.-M. 2009, *PASJ*, 61, 1165 (Paper I)
- Takeda, Y., Kang, D.-I., Han, I., Lee, B.-C., Kim, K.-M., Kawanomoto, S., & Ohishi, N. 2012, *PASJ*, 64, 38 (Paper II)
- Takeda, Y., & Sadakane, K. 1997, *PASJ*, 49, 367
- Takeda, Y., Takada-Hidai, M., Jugaku, J., Sakaue, A., & Sadakane, K. 1999, *PASJ*, 51, 961

Talon, S., Richard, O., & Michaud, G. 2006, ApJ, 645, 634

van Leeuwen, F. 2007, Hipparcos, the New Reduction of the Raw Data (Berlin: Springer)

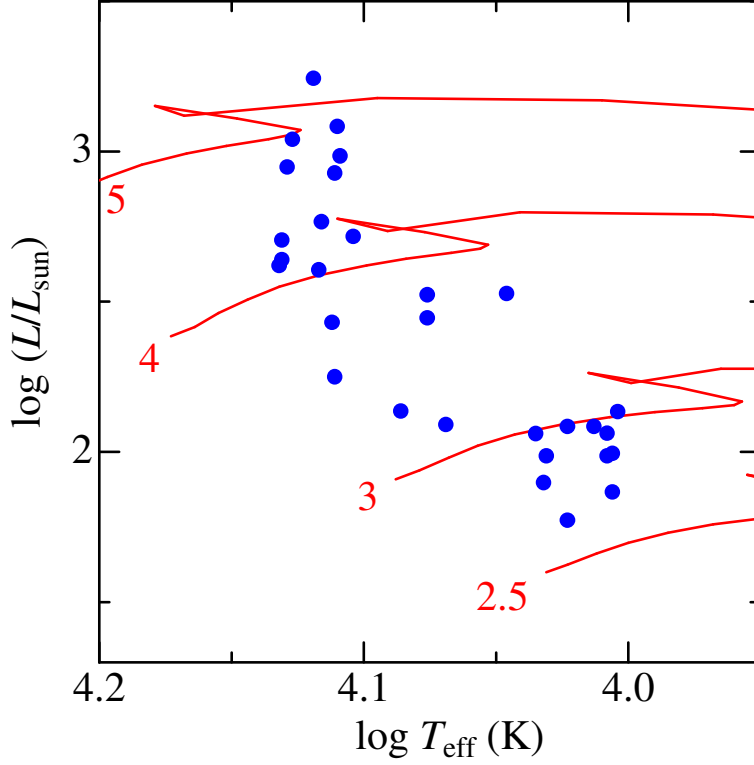


Fig. 1. Plots of the 30 program stars on the theoretical HR diagram ($\log(L/L_{\odot})$ vs. $\log T_{\text{eff}}$), where the effective temperature (T_{eff}) was determined from *wby β* photometry as described in section 3 and the bolometric luminosity (L) was evaluated from the apparent visual magnitude, Hipparcos parallax (van Leeuwen 2007), Arenou et al.’s (1992) interstellar extinction map, and Flower’s (1996) bolometric correction. Theoretical evolutionary tracks corresponding to the solar metallicity computed by Girardi et al. (2000) for four different initial masses (2.5, 3, 4, and 5 M_{\odot}) are also depicted for comparison.

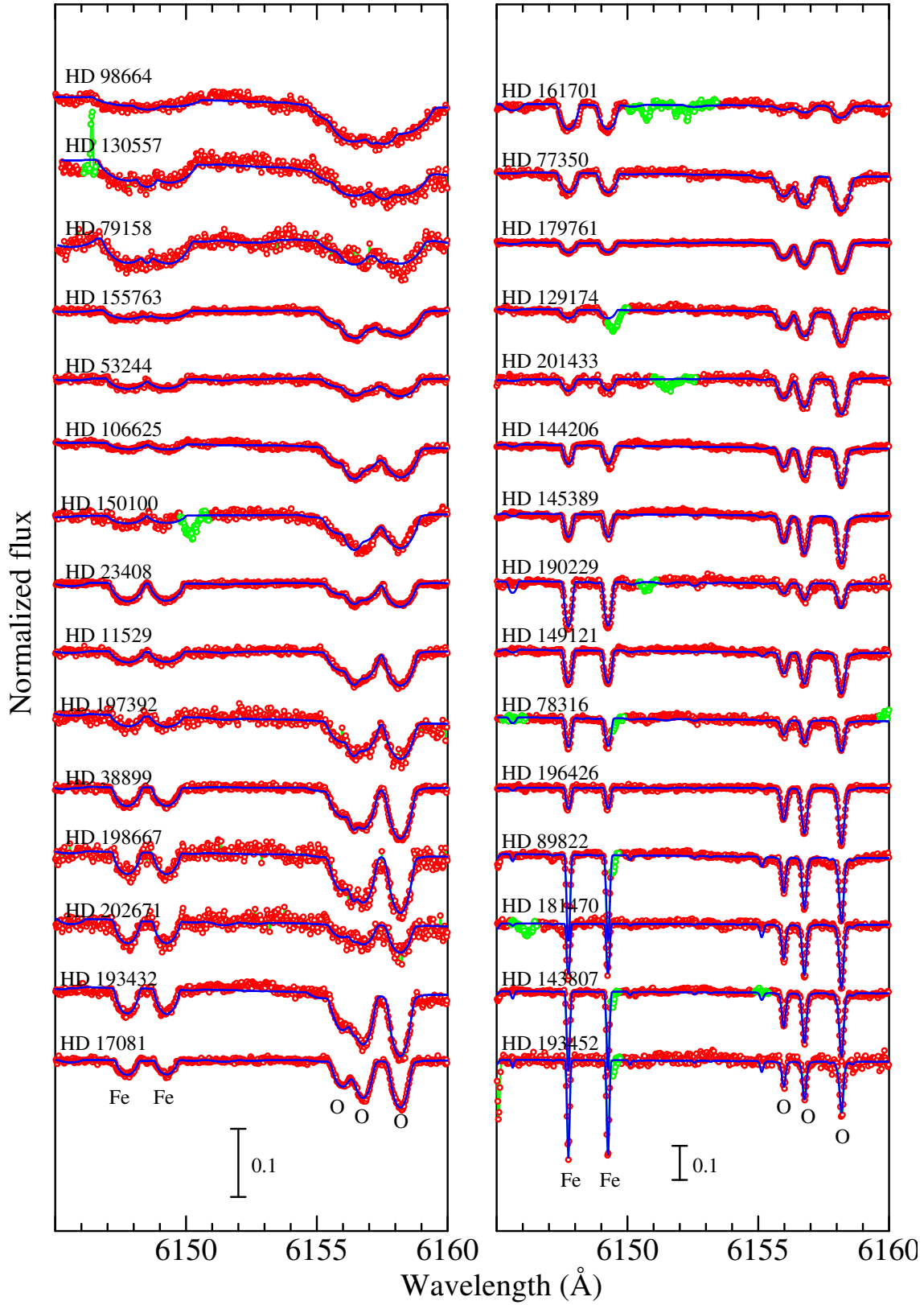


Fig. 2. Synthetic spectrum fitting in the 6145–6160 Å region accomplished by varying $v_e \sin i$, A^{O} , and A^{Fe} . The best-fit theoretical spectra are shown by blue solid lines. The observed data are plotted by symbols, where those due to stellar origin and actually used in fitting are depicted in red, while those of non-stellar origin and rejected in fitting are highlighted in green. The spectra are arranged (from top to bottom) in the descending order of $v_e \sin i$ as in table 1, and offset values of 0.1 (left panel) and 0.2 (right panel) are applied to each spectrum relative to the adjacent one.

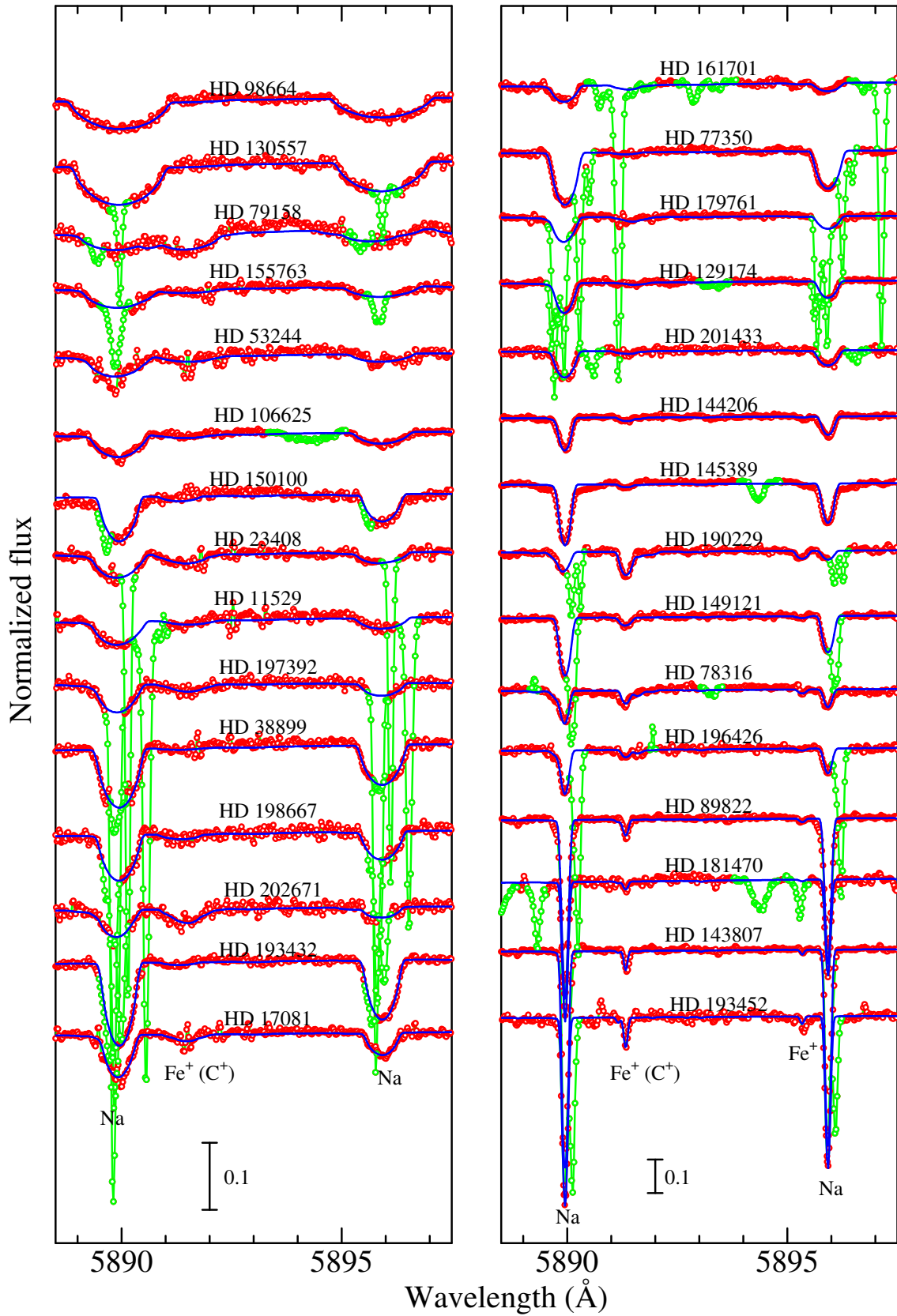


Fig. 3. Synthetic spectrum fitting in the 5888.5–5897.5 Å region accomplished by varying A^{Na} and A^{Fe} . Note that this spectral region tends to be severely contaminated by sharp interstellar Na I lines, which had to be masked in the fitting. Otherwise, the same as in figure 2.

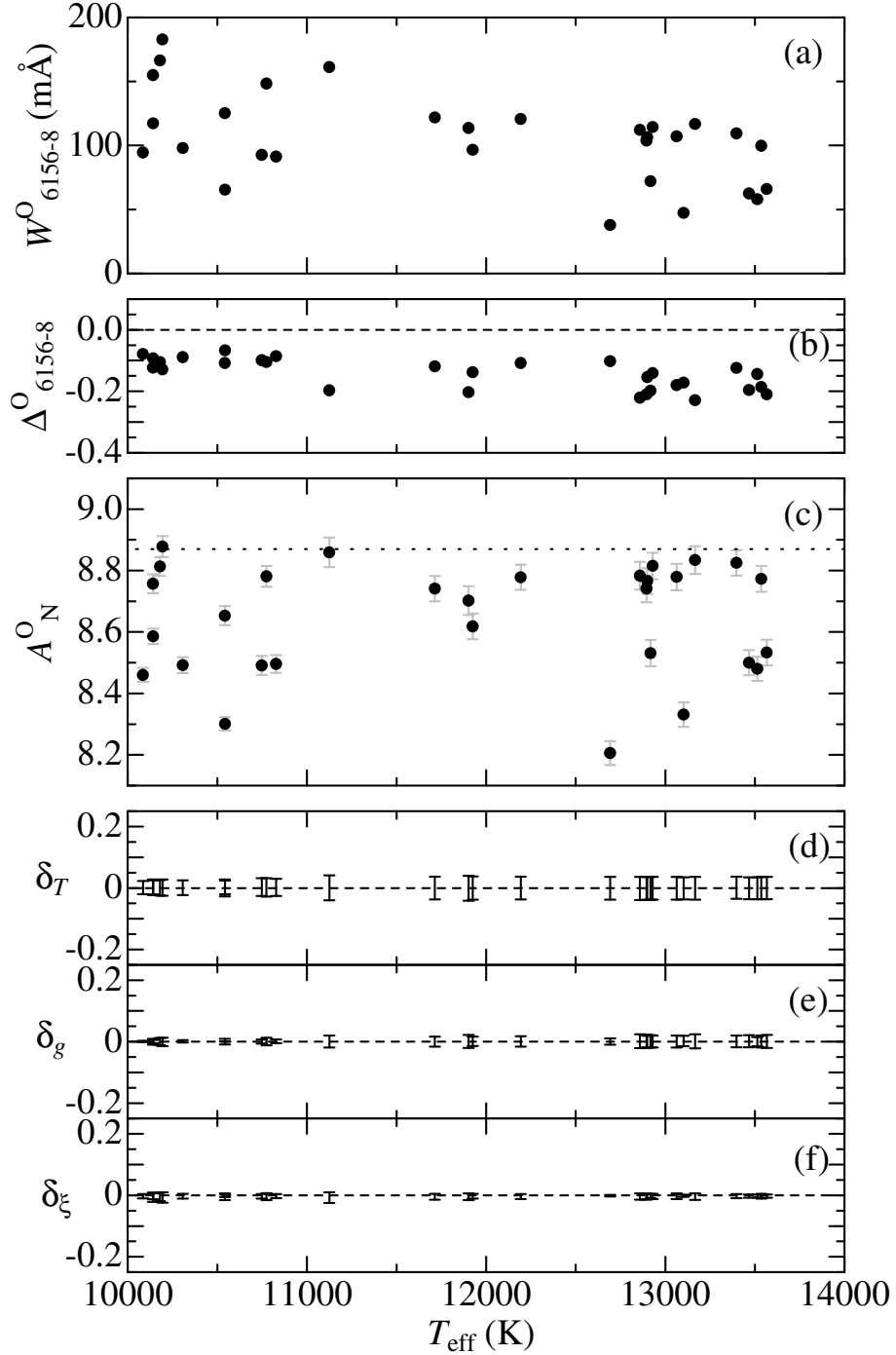


Fig. 4. Oxygen abundances along with the abundance-related quantities specific to the O I 6156–6158 triplet feature, plotted against T_{eff} . (a) W_{6156-8}^{O} (equivalent width), (b) $\Delta_{6156-8}^{\text{O}}$ (non-LTE correction), (c) A_{N}^{O} (non-LTE oxygen abundance, where the attached error bar is $\delta_{Tg\xi}$ defined in subsection 4.2), (d) δ_{T+} and δ_{T-} (abundance variations in response to T_{eff} changes of +3% and –3%), (e) δ_{g+} and δ_{g-} (abundance variations in response to $\log g$ changes of +0.2 dex and –0.2 dex), and (f) $\delta_{\xi+}$ and $\delta_{\xi-}$ (abundance variations in response to perturbing the standard $\xi = 1 \text{ km s}^{-1}$ by +1 km s^{-1} and –1 km s^{-1}). The signs of δ 's are $\delta_{T+} > 0$, $\delta_{T-} < 0$, $\delta_{g+} < 0$, $\delta_{g-} > 0$, $\delta_{\xi+} < 0$, and $\delta_{\xi-} > 0$. The horizontal dotted line in panel (c) indicates the reference solar abundance (cf. the caption in figure 7).

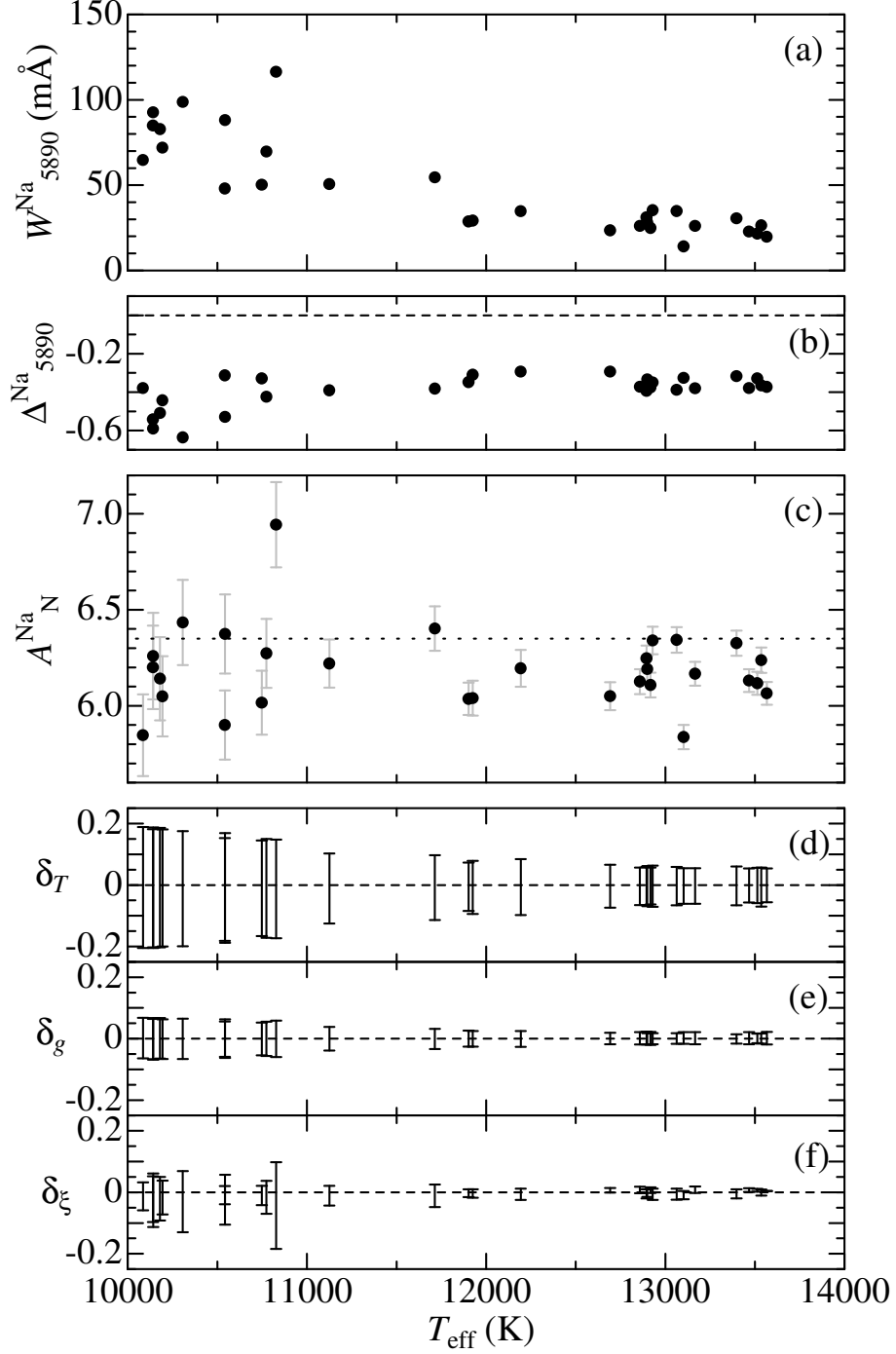


Fig. 5. Sodium abundances along with the abundance-related quantities specific to the Na I 5890 line, plotted against T_{eff} . (a) W_{5890}^{Na} (equivalent width), (b) $\Delta_{5890}^{\text{Na}}$ (non-LTE correction), (c) A_{N}^{Na} (non-LTE sodium abundance), (d) δ_{T+} and δ_{T-} (abundance variations in response to changing T_{eff}), (e) δ_{g+} and δ_{g-} (abundance variations in response to changing $\log g$ changes), and (f) $\delta_{\xi+}$ and $\delta_{\xi-}$ (abundance variations in response to changing ξ). The signs of δ 's are $\delta_{T+} > 0$, $\delta_{T-} < 0$, $\delta_{g+} < 0$, $\delta_{g-} > 0$, $\delta_{\xi+} < 0$, and $\delta_{\xi-} > 0$. Otherwise, the same as figure 4.

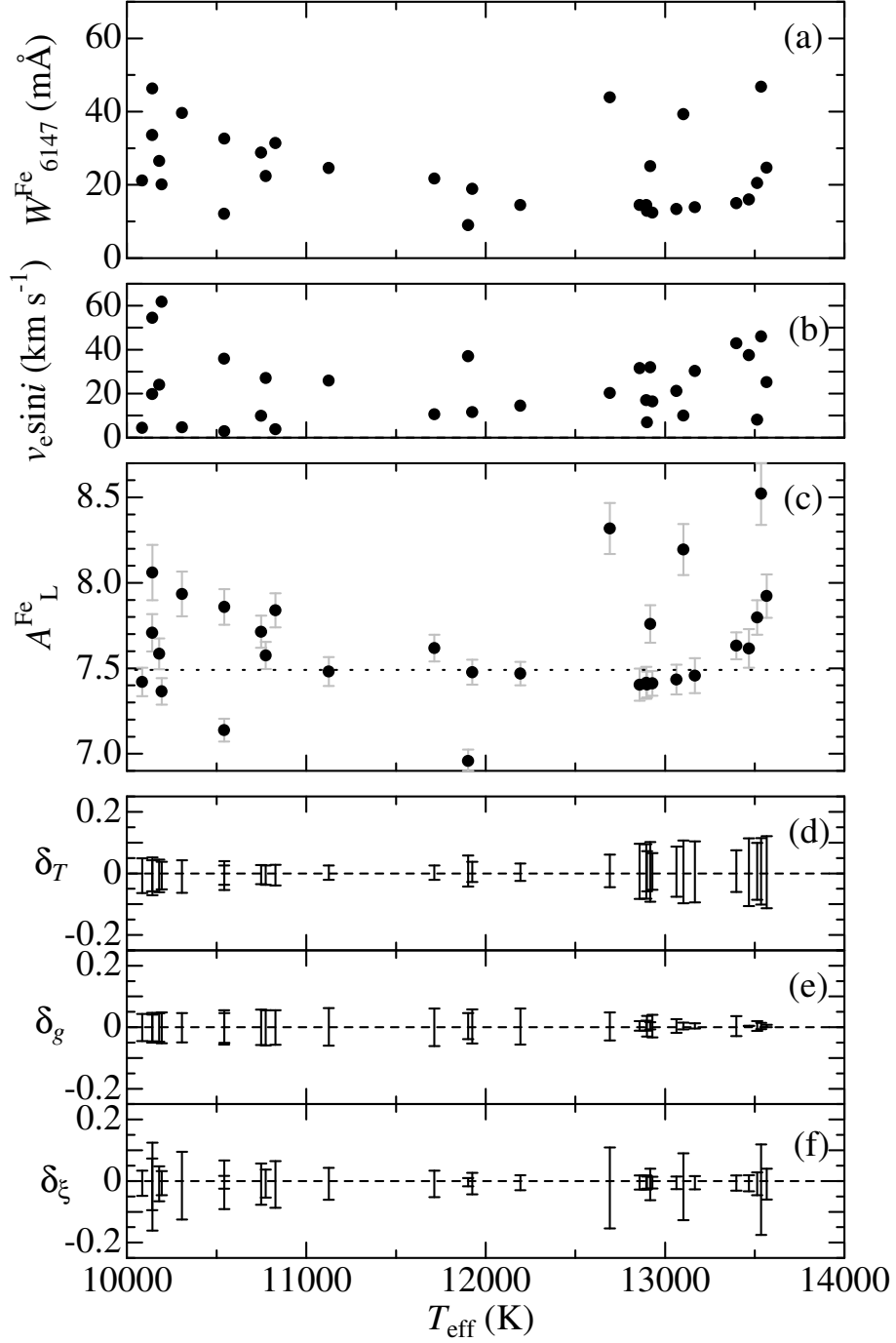


Fig. 6. Iron abundances along with the abundance-related quantities specific to the Fe II 6147 line, plotted against T_{eff} . (a) W_{6147}^{Fe} (equivalent width), (b) $v_e \sin i$ (projected rotational velocity), (c) A_L^{Fe} (LTE iron abundance), (d) δ_{T+} and δ_{T-} (abundance variations in response to changing T_{eff}), (e) δ_{g+} and δ_{g-} (abundance variations in response to changing $\log g$ changes), and (f) $\delta_{\xi+}$ and $\delta_{\xi-}$ (abundance variations in response to changing ξ). The signs of δ 's are $\delta_{T+} > 0$, $\delta_{T-} < 0$, $\delta_{g+} > 0$, $\delta_{g-} < 0$, $\delta_{\xi+} < 0$, and $\delta_{\xi-} > 0$. Otherwise, the same as figure 4.

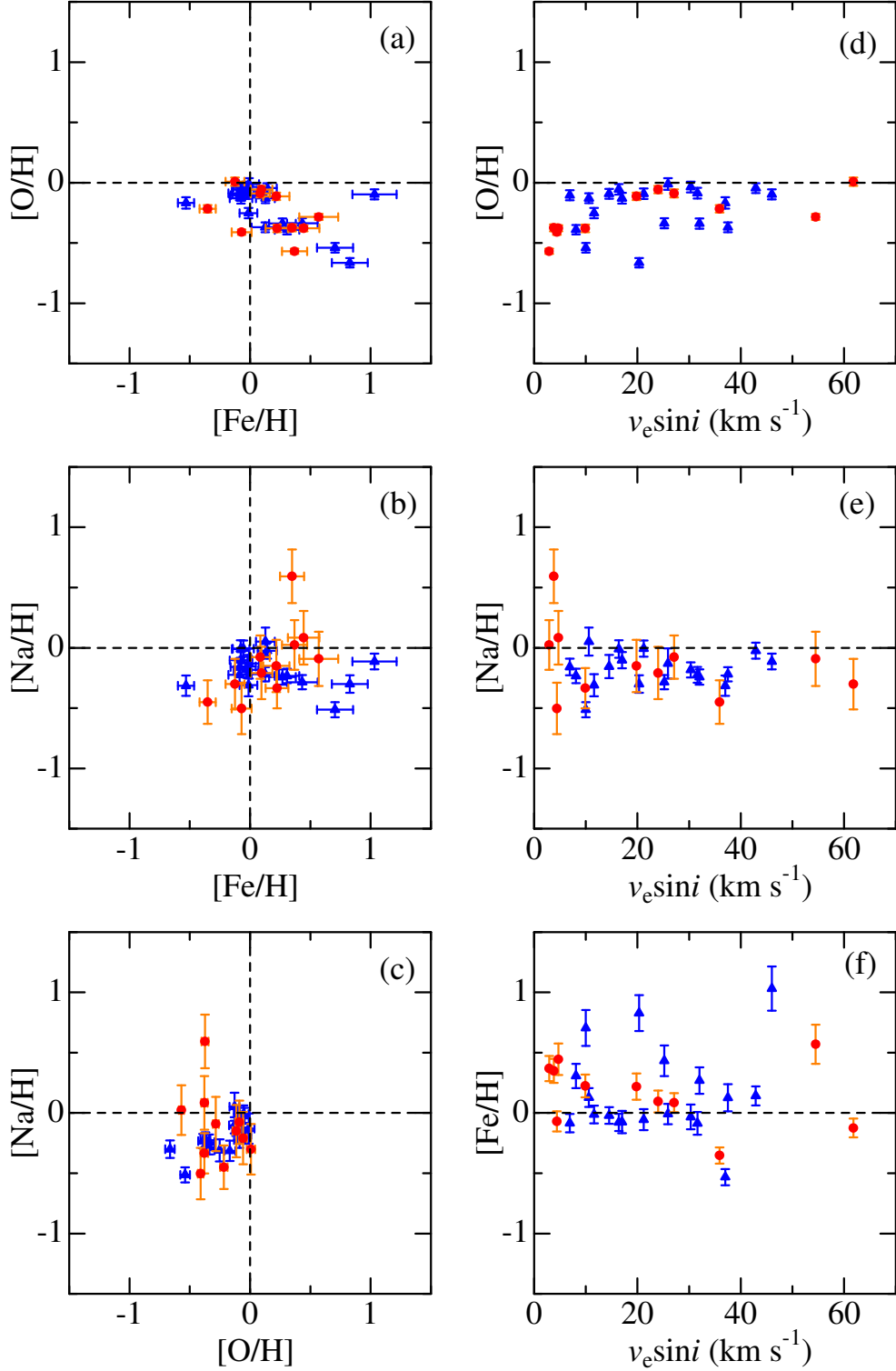


Fig. 7. Left panels show the correlations between [O/H], [Na/H], and [Fe/H]: (a) [O/H] vs. [Fe/H], (b) [Na/H] vs. [Fe/H], and (c) [Na/H] vs. [O/H]. In right panels (d), (e), and (f), [O/H], [Na/H], and [Fe/H] are plotted against $v_e \sin i$, respectively. Circles (red) and triangles (blue) correspond the results for stars with $T_{\text{eff}} < 11000$ K and those with $T_{\text{eff}} > 11000$ K, respectively. In evaluating $[X/H] (\equiv A_{\text{star}}^X - A_{\text{sun}}^X)$, we adopted $A_{\text{sun}}^{\text{O}} = 8.87$, $A_{\text{sun}}^{\text{Na}} = 6.35$, and $A_{\text{sun}}^{\text{Fe}} = 7.49$, for which the abundances of Procyon (known to be almost of solar composition) derived from the same lines were substituted (cf. Takeda et al. 2008, Paper I).

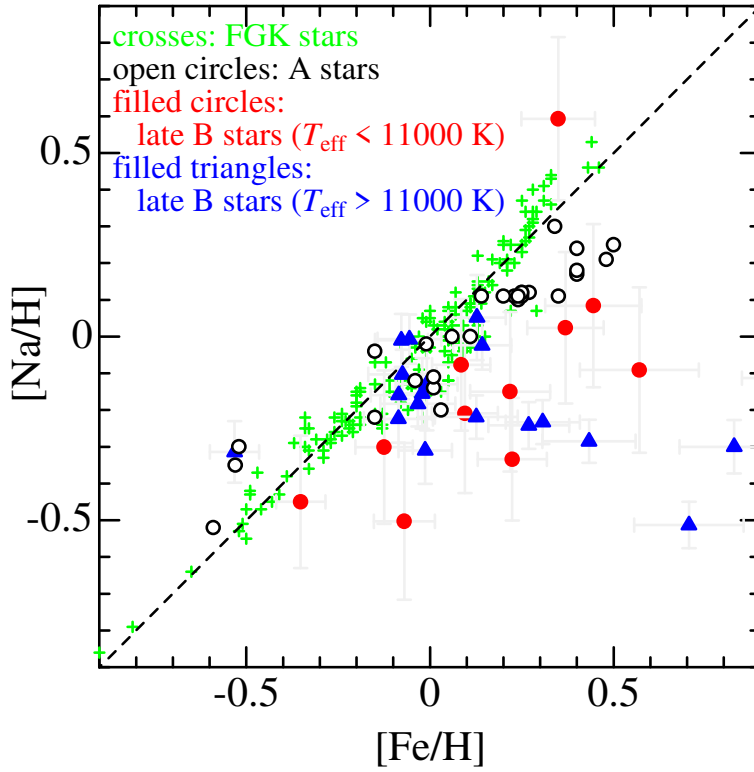


Fig. 8. Combined $[\text{Na}/\text{H}]$ vs. $[\text{Fe}/\text{H}]$ correlations for stars of different spectral types. Crosses \dots FGK stars (Takeda 2007), open circles \dots sharp-lined A-type stars (Paper II), filled circles \dots late B-type stars with $T_{\text{eff}} < 11000$ K (this study), and filled triangles \dots late B-type stars with $T_{\text{eff}} > 11000$ K (this study).

Table 1. Basic data of the program stars and the results of the analysis.

HD#	Desig.	Sp.type	T_{eff}	$\log g$	$v_e \sin i$	W_{6156-8}^{O}	A_{N}^{O}	$\Delta_{6156-8}^{\text{O}}$	W_{5890}^{Na}	A_{N}^{Na}	$\Delta_{5890}^{\text{Na}}$	W_{6147}^{Fe}	A_{L}^{Fe}	Obs. date
098664	σ Leo	B9.5Vs	10194	3.75	62	183	8.88	-0.13	72	6.05	-0.44	20	7.37	2012 May 31
130557	HR 5522	B9Vsvar...	10142	3.85	55	117	8.59	-0.09	93	6.26	-0.59	46	8.06	2012 May 31
079158	36 Lyn	B8IIIMNp	13535	3.72	46	100	8.77	-0.19	26	6.24	-0.37	47	8.52	2012 May 31
155763	ζ Dra	B6III	13397	4.24	43	109	8.83	-0.12	31	6.33	-0.32	15	7.63	2006 Oct 23
053244	γ CMa	B8II	13467	3.42	38	63	8.50	-0.20	23	6.13	-0.38	16	7.62	2006 Oct 23
106625	γ Crv	B8III	11902	3.36	37	114	8.70	-0.20	29	6.04	-0.35	9	6.96	2012 May 27
150100	16 Dra	B9.5Vn	10542	3.84	36	125	8.65	-0.11	48	5.90	-0.31	12	7.14	2012 May 31
023408	20 Tau	B8III	12917	3.36	32	72	8.53	-0.20	25	6.11	-0.38	25	7.76	2006 Oct 23
011529	46 Cas	B8III	12858	3.43	32	112	8.78	-0.22	26	6.13	-0.37	15	7.40	2006 Oct 23
197392	HR 7926	B8II-III	13166	3.46	30	117	8.83	-0.23	26	6.17	-0.38	14	7.46	2012 May 29
038899	134 Tau	B9IV	10774	4.02	27	148	8.78	-0.11	70	6.27	-0.42	22	7.58	2006 Oct 23
198667	5 Aqr	B9III	11125	3.42	26	161	8.86	-0.20	51	6.22	-0.39	25	7.48	2012 May 28
202671	30 Cap	B5II/III	13566	3.36	25	66	8.53	-0.21	20	6.07	-0.37	25	7.92	2012 May 31
193432	ν Cap	B9IV	10180	3.91	24	166	8.81	-0.11	83	6.14	-0.51	27	7.59	2012 May 26
017081	π Cet	B7IV	13063	3.72	21	107	8.78	-0.18	35	6.34	-0.39	13	7.43	2006 Oct 20
161701	HR 6620	B9V	12692	4.04	20	38	8.21	-0.10	24	6.05	-0.29	44	8.32	2012 May 27
077350	ν Cnc	A0III	10141	3.68	20	155	8.76	-0.12	85	6.20	-0.54	34	7.71	2012 May 27
179761	21 Aql	B8II-III	12895	3.46	17	104	8.74	-0.21	31	6.25	-0.39	15	7.42	2006 Oct 21
129174	π^1 Boo	B9p MnHg	12929	4.02	16	114	8.82	-0.14	35	6.34	-0.35	12	7.41	2012 May 26
201433	HR 8094	B9V	12193	4.24	15	121	8.78	-0.11	35	6.20	-0.29	15	7.47	2012 May 28
144206	ν Her	B9III	11925	3.79	12	97	8.62	-0.14	29	6.04	-0.31	19	7.48	2012 May 27
145389	ϕ Her	B9MNp...	11714	4.02	11	122	8.74	-0.12	55	6.40	-0.38	22	7.62	2012 May 27
190229	14 Sge	B9MNp...	13102	3.46	10	47	8.33	-0.17	14	5.84	-0.33	39	8.20	2012 May 28
149121	28 Her	B9.5III	10748	3.89	10	93	8.49	-0.10	50	6.02	-0.33	29	7.71	2012 May 27
078316	κ Cnc	B8IIIMNp	13513	3.85	8	58	8.48	-0.14	22	6.12	-0.33	21	7.80	2012 May 28
196426	HR 7878	B8IIp	12899	3.89	7	106	8.77	-0.15	28	6.19	-0.33	13	7.41	2006 Oct 21
089822	HR 4072	A0sp...	10307	3.89	5	98	8.49	-0.09	99	6.43	-0.64	40	7.94	2012 May 27
181470	HR 7338	A0III	10085	3.92	4	95	8.46	-0.08	65	5.85	-0.38	21	7.42	2006 Oct 21
143807	ι CrB	A0p...	10828	4.06	4	91	8.50	-0.09	116	6.94	-0.71	31	7.84	2012 May 26
193452	HR 7775	B9.5III/IV	10543	4.15	3	65	8.30	-0.07	88	6.37	-0.53	33	7.86	2012 May 29

Note.

In columns 1 through 6 are given the HD number, star designation, spectral type (taken from Hipparcos catalogue), effective temperature (in K), logarithmic surface gravity (in cm s^{-2}), and projected rotational velocity (in km s^{-1} ; from 6145–6160 Å fitting). Columns 7 through 14 show the results of abundance analyses: merged equivalent width of the O I 6156–8 lines, non-LTE O abundance and NLTE correction; equivalent width of the Na I 5890 line, non-LTE Na abundance, and NLTE correction; equivalent width of the Fe II 6147 line and (LTE) Fe abundance. Finally, column 15 gives the observation date. All abundance results are expressed in the usual normalization of $A^{\text{H}} = 12.00$. The objects are arranged in the descending order of $v_e \sin i$.

Table 2. Atomic data of important lines relevant to the analysis.

Desig.	Species	RMT	$\lambda(\text{\AA})$	χ_{low} (eV)	$\log gf$
6156	O I	10	6155.961	10.74	-1.40
	O I	10	6155.971	10.74	-1.05
	O I	10	6155.989	10.74	-1.16
6157	O I	10	6156.737	10.74	-1.52
	O I	10	6156.755	10.74	-0.93
	O I	10	6156.778	10.74	-0.73
6158	O I	10	6158.149	10.74	-1.89
	O I	10	6158.172	10.74	-1.03
	O I	10	6158.187	10.74	-0.44
5890	Na I	1	5889.951	0.00	+0.12
5896	Na I	1	5895.924	0.00	-0.18
6147	Fe II	74	6147.741	3.89	-2.72
6149	Fe II	74	6149.258	3.89	-2.72

Note.

All data are were taken from Kurucz & Bell's (1995) compilation. RMT is the multiplet number in the Revised Multiplet Table (Moore 1959).

Table 3. Statistical trend of correlation between Na and Fe for each group of different T_{eff} .

Source	Sp. type	T_{eff} range	N	r	m	b	σ	Remark
Takeda (2007)	FGK	5000–7000 K	159	+0.962	+1.031(± 0.023)	-0.016(± 0.006)	0.078	
Paper II	A	7000–10000 K	28	+0.945	+0.641(± 0.043)	-0.056(± 0.013)	0.065	
This study	late B (near A0)	10000–11000 K	10	+0.782	+0.546(± 0.154)	-0.280(± 0.047)	0.122	HD 143807 (outlier) excluded
This study	late B	11000–14000 K	19	-0.267	-0.097(± 0.085)	-0.167(± 0.034)	0.131	
	<i>late B (subdivided)</i>	<i>11000–13000 K</i>	<i>11</i>	<i>-0.085</i>	<i>-0.032(± 0.123)</i>	<i>-0.171(± 0.039)</i>	<i>0.121</i>	
	<i>late B (subdivided)</i>	<i>13000–14000 K</i>	<i>8</i>	<i>-0.407</i>	<i>-0.174(± 0.159)</i>	<i>-0.139(± 0.077)</i>	<i>0.148</i>	

Note.

See figure 8 for graphical representations of Na vs. Fe correlations for each group. The last two lines (printed in *italic* type) show the results for the two subdivided groups of the $T_{\text{eff}} = 11000\text{--}14000$ K stars given in the 4th line. N is the number of stars, and r is the correlation coefficient between $[\text{Na}/\text{H}]$ and $[\text{Fe}/\text{H}]$. m and b are the coefficients of the linear regression line ($[\text{Na}/\text{H}] = m [\text{Fe}/\text{H}] + b$) determine by the least squares analysis (standard errors of m and b are also given in parentheses with \pm), while σ is the standard deviation of the residual between the actual values of $[\text{Na}/\text{H}]$ and those computed from this linear relation.